HOKKAIDO UNIVERSITY

Title	Arrhythmogenic β-adrenergic signaling in cardiac hypertrophy : The role of small-conductance calcium-activated potassium channels via activation of CaMKII
Author(s)	Kamada, Rui; Yokoshiki, Hisashi; Mitsuyama, Hirofumi et al.
Citation	European journal of pharmacology, 844, 110-117 https://doi.org/10.1016/j.ejphar.2018.12.011
Issue Date	2019-02-05
Doc URL	https://hdl.handle.net/2115/76694
Rights	© 2019. This manuscript version is made available under the CC-BY-NC-ND 4.0 license http://creativecommons.org/licenses/by-nc-nd/4.0/
Rights(URL)	https://creativecommons.org/licenses/by-nc-nd/4.0/
Type	journal article
File Information	EurJPharmacol844_110.pdf

Hokkaido University Collection of Scholarly and Academic Papers : HUSCAP

Arrhythmogenic β-adrenergic signaling in cardiac hypertrophy: the role of small-conductance calcium-activated potassium channels via activation of CaMKII

Rui Kamada[*1], Hisashi Yokoshiki [*2], Hirofumi Mitsuyama [*1], Masaya Watanabe [*1], Kazuya Mizukami [*3], Taro Tenma [*1], Masayuki Takahashi, [*1], Shingo Takada, [*1], and - Toshihisa Anzai[*1]

[*1] Department of Cardiovascular Medicine, Hokkaido University Graduate School of Medicine;

[*2] Department of Cardiovascular Medicine, Sapporo City General Hospital;

[*3] Department of Cardiovascular Medicine, National Hospital Organization Hokkaido Medical Center

Correspondence: Hisashi Yokoshiki MD, PhD

Department of Cardiovascular Medicine, Sapporo City General Hospital, Kita-11, Nishi-13, Chuo-ku, Sapporo 060-8604, Japan.

Phone: +81-11-726-2211; Fax: +81-11-726-7912

E-mail: hisashi.yokoshiki@doc.city.sapporo.jp

Abstracts

Sustained ventricular arrhythmias (SVAs) lead to sudden cardiac death, for which β-adrenoreceptor blockers are effective. We hypothesized that electrophysiological changes and arrhythmias by β- adrenoreceptor stimulation are crucially related to activation of small-conductance calcium-activated potassium (SK) channels via the increase in Ca^{2+} / calmodulin-dependent protein kinase II (CaMKII) activity. We used normotensive Wistar-Kyoto (WKY) rats and spontaneous hypertensive rats (SHRs). The latter served as a model of left ventricular hypertrophy. We performed dual optical mapping of action potentials and Ca^{2+} transients, and the effects of isoproterenol and apamin, an SK channel blocker, were evaluated in the Langendorff-perfused hearts. Action potential duration was abbreviated by isoproterenol (100 nM) in both WKY rats and SHRs. In contrast, the CaMKII activity was increased by isoproterenol only in SHRs. In the presence of isoproterenol, apamin prolonged the action potential duration only in SHRs (n = 10, from 116.6 ± 5.05 ms to 125.4 ± 3.80 ms, P = 0.011), which was prevented by KN-93, a CaMKII inhibitor. Increase in Ca^{2+} transients and shortening of Ca^{2+} transient duration by isoproterenol were similarly observed in both animals, which was not affected by apamin. Apamin reduced the isoproterenol-induced SVAs and maximal slope of action potential duration restitution curve specifically in SHRs. In

conclusion, β- adrenoreceptor stimulation creates arrhythmogenic substrates via the CaMKII-dependent activation of SK channels in cardiac hypertrophy.

Key words: SK channels, β- adrenoreceptor stimulation, CaMKII, Cardiac hypertrophy, Rat

1. Introduction

β-adrenoreceptor stimulation is known to increase ventricular tachyarrhythmias (Han et al., 1964; Meredith et al., 1991) , thereby leading to sudden cardiac death. In experimental animals, β- adrenoreceptor stimulation increased diastolic Ca^{2+} leak from sarcoplasmic reticulum (SR) via the CaMKII activation (Curran et al., 2007) and abbreviated action potential duration (APD) as well as effective refractory period (ERP) (Litovsky and Antzelevitch, 1990) . Recently, it was also reported that acute β-adrenoreceptor stimulation significantly abbreviated APD in human failing hearts (Lang et al., 2015) . However, little is known about the relationship between these electrophysiological changes and the arrhythmogenic β- adrenoreceptor signaling.

Small-conductance calcium-activated potassium channels (SK channels) belong to a group of potassium-selective and voltage-independent ion channels (Adelman et al., 2012) . SK channels have a high calcium-sensitivity, and exist in various tissues including hearts (Adelman et al., 2012). It was reported that SK channels had a little contribution to the ventricular repolarization during action potentials of normal hearts (Nagy et al., 2009) . In contrast, in failing and hypertrophied hearts, these channels played an important role in the ventricular repolarization (Chua et al., 2011; Mizukami et al., 2015). We also reported that SK channels were upregulated via

activation of CaMKII in hypertrophied rat hearts (Mitsuyama et al., 2014; Mizukami et al., 2015). At present, it is not well known that activation of SK channels produces anti-arrhythmic or proarrhythmic functions (Chang et al., 2013; Chua et al., 2011). Therefore, we hypothesized that the CaMKII activation through β- adrenoreceptor stimulation could regulate the opening of SK channels and induce arrhythmogenesis in cardiac hypertrophy.

2. Materials and Methods

2.1. Ethical Approval

The research protocol was conformed to animal care guidelines for the Care and Use of Laboratory Animals in Hokkaido University Graduate School of Medicine, and was approved by our institutional animal research committee.

2.2. Drugs

Isoproterenol hydrocloride, N-[4-[1-[2-(6-methylpyridin-2-yl)ethyl]piperidine-4-carbonyl]phenyl]methanesulfonamide (E4031), pyridine-4-amine (4-AP) were purchased from Sigma-Aldrich (MO, USA). Apamin was purchased from PEPTIDE (Osaka, Japan). KN93 was purchased from Millipore (MA, USA). Blebbistatin was purchased from Toronto Research Chemicals (Toronto, Canada). We used dimethyl sulfoxide (DMSO) as a solvent for various drugs, with a final concentration of 0.1% to 0.5%.

2.3. Experimental preparation

Male 18- to 27-week-old Wister-Kyoto rats (WKY) and spontaneous hypertensive rats (SHRs) were used. SHRs at these ages are known to have established

cardiac hypertrophy without any systolic dysfunction or heart failure (Chan et al., 2011). All animals were anesthetized with inhalation with diethyl ether (Nacalai tesque, Kyoto, Japan) and with intraperitoneal injection of the mixture which was made from medetomidine hydrochloride (0.15 mg/kg; Kyoritsu Seiyaku, Tokyo, Japan), midazolam (2 mg/kg; Astellas Pharma, Tokyo, Japan) and butorphanol (2.5 mg/kg; Meiji Seika Pharma, Tokyo, Japan) (Kirihara et al., 2016). Subsequently, heparin sodium (400 IU/kg) was interperitoneally injected. The hearts were quickly excised and perfused with Langendorff apparatus with oxygenated (100% O_2) Tyrode solution (37 °C) containing (in mM) 143 NaCl, 5.4 KCl, 0.33 NaH_2PO_4, 5 HEPES, 5.5 glucose, 0.5 $MgCl_2$, and 1.8 $CaCl_2$ (pH 7.4 adjusted using NaOH) until the heart rate became stable state. The perfusion pressure was kept at 70 cm H_2O for WKY and 100 cm H_2O for SHR to adjust coronary flow per heart weight, as described previously (Kohya et al., 1995). A unipolar pacing electrode was attached to the left ventricular (LV) apex, and two electrodes were attached to left ventricle and right ventricle to record the electrogram (EG). Perfused hearts were immobilized by an inhibitor of myosin II, blebbistatin (10 μM, TRC, Toronto, Canada), and stained with a voltage-sensitive fluorescence dye, RH237 (0.01 μM, Molecular Probes, OR, USA), and a Ca^{2+}-sensitive dye, Rhod-2 AM (1.0 μM, DOJINDO, Kumamoto, Japan, containing 20% wt/vol

Pluronic F-127).

2.4. Dual optical mapping

We simultaneously mapped calcium transient (CaT) and action potential (AP) as previously described (Maruyama et al., 2010). We prepared 1mg of Rhod-2AM dissolved in 0.93ml of dimethyl sulfoxide containing Pluronic F-127 (20% wt/vol) to stain intracellular calcium, as stock solution. This solution, diluted in 100 ml of Tyrode solution to achieve a final Rhod-2AM concentration of 1 μM, was infused into the heart for 10 min. For membrane potential staining, voltage sensitive dye RH-237 dissolved in dimethyl sulfoxide (0.2 μM) was directly injected into the Langendorff perfusion system. The voltage sensitive dye and calcium sensitive dye were illuminated using a 531 ± 20-nm light emitted by a 150-W halogen light source. The fluorescence was filtered through a common lens, separated with a dichroic mirror (662 nm cutoff wavelength). It was filtered with the 715 nm longpass filter for V_m and a 575 ± 7.5 nm bandpass filter for Ca_i and recorded with charge-coupled device camera (MiCAM02, Brain Vision, Tokyo, Japan) at 0.2-mm spatial (88 × 60 pixels) and 2.2-ms temporal resolutions. We performed dual optical mappings of anterior epicardial surface of LV. The 3 × 3 spatial and cubic filters were used to minimize the post-acquisition artifacts.

Optical APDs and calcium transient durations (CaTDs) were measured at 90% repolarization and recovery (APD_{90}, $CaTD_{90}$) respectively. Atrial signals, the pixels with inadequate action potentials and at the edge of LV were excluded. We obtained the median APD_{90} and $CaTD_{90}$ out of the all available APD_{90} and $CaTD_{90}$ and defined them as the individual APD_{90} and $CaTD_{90}$.

2.5. Experimental protocol

We measured the baseline action potentials and calcium transients with a pacing cycle length of 200 ms using the dual optical mapping. Then, isoproterenol (100 nM, Sigma-Aldrich, MO, USA) was perfused for 10 min. After that, apamin (100 nM, PEPTIDE, Osaka, Japan) was perfused for10 min in the presence of isoproterenol. In the SHR group, KN93 (1 μM, Millipore, MA, USA), an inhibitor of CaMKII, was added to the perfusate in the presence of isoproterenol or isoproterenol plus apamin.

2.6. Induction of arrhythmia

We first assessed the inducibility of arrhythmias in the Langendorff-perfused hearts from WKY rats and SHRs in the absence (control) and presence of isoproterenol. During the induction protocols, ventricular electrograms were recorded continuously.

Subsequently, we evaluated the effects of apamin, an SK channel blocker, on the arrhythmogenesis produced by isoproterenol in both animals. Hearts were paced from LV apex at twice diastolic threshold current with a silver unipolar electrode at a pacing cycle length of 200 ms. After that, the pacing cycle length was shortened (reduced in 10-ms steps each 10 beats) until the ventricular arrhythmias were induced or 1:1 capture was lost. We defined a premature electrical complex arising below the atrioventricular node as a ventricular arrhythmia (VA). A VA was seen as a premature ventricular electrical complex that is different in shape (voltage and/or duration) from the inherent ventricular complex. We defined ventricular tachycardia (VT) as a run of four or more consecutive VAs. And, we distinguished monomorphic VT from polymorphic VT based on the shape of ventricular complex. During monomorphic VT, the shape was constant. If the shape changed sequentially in consecutive complexes, we defined it as polymorphic VT. Ventricular fibrillation (VF) was defined as a rhythm in which successive complexes all varied non-progressively, that is, independently or chaotically (Curtis et al., 2013). If any of these arrhythmias (monomorphic VT, polymorphic VT, and VF) lasted more than 10 s, we described it as a sustained ventricular arrhythmia (SVA).

2.7. CaMKII activity

Isolated rat hearts were perfused for 15 min with either standard Tyrode solution or Tyrode solution containing isoproterenol (100 nM) during pacing at the cycle length of 180 ms. Left ventricular tissue was fast frozen in liquid nitrogen and stored -80°C until the time of assay. Left ventricular tissue was homogenized on ice in cell RIPA Lysis Buffer System (Santa Cruz Biotechnology, TX, USA) supplemented with a protease inhibitor cocktail, phenyl methyl sulfonyl fluoride, and sodium orthovanadate in water. After centrifugation at 15000 *g* for 20 min at 4°C, supernatants were collected for CaMKII activity measurement. The protein concentration was quantified by the BCA Protein Assay (Thermo sientific, IL, USA). CaM-kinase II Assay Kit (MEDICAL & BIOLOGICAL LABORATORIES, MA, USA) was used to quantify CaMKII activity by loading 1.0 μg/μl protein in each well with a reaction mixture without (to measure basal autophosphorylated CaMKII activity) or with saturating Ca^{2+}/calmodulin (to measure maximal activity) (Pezhouman et al., 2015). All assay was incubated for 30 min at 30°C. After washing all assay, horseradish peroxidase conjugated anti-phospho-Syntide-2 antibody was added and incubated for 60 minutes at room temperature. After washing, 100 ul of substrate reagent was added and incubated for 10 minutes at room temperature, followed by 100 μl of stop solution. All assay was

measured absorbance at 450 nm. CaMKII positive control (Cyclex Co Ltd) was used for standard curve preparation. We measured the tissue level of CaMKII activity at both basal and isoproterenol-stimulated conditions, as the ratio of maximal CaMKII activity.

2.8. APD restitution curve

A standard dynamic pacing protocol was performed to measure APD restitution (Goldhaber et al., 2005). Isolated rat hearts were paced at a cycle length of 200 ms. Thereafter, the cycle length was decreased by 5 to 10 ms every 8 seconds, until 1:1 capture loss or an SVA occurred. The APD_{90} was defined as the 90% repolarization duration. Diastolic interval (DI) was defined as cycle length minus APD_{90}. APD restitution curves were constructed by plotting APD_{90} versus DI in control, the presence of ISO and ISO plus apamin. In SHRs, we measured APD restitution curves in the presence of 4 – aminopyridine (1mM, Sigma – Aldrich, MO, USA) (4-AP), a blocker of transient outward currents (I_{to}), and the presence of E-4031(1 μ M, Sigma – Aldrich, MO, USA), a blocker of rapid delayed rectifier currents (I_{Kr}). The data points were fitted to a single exponential curve. The maximum APD restitution slope was calculated from the first derivative of the fitted exponential curve.

2.9. Statistical analysis

All data are reported as means ± S.E.M. Statistical differences of the means between two groups were determined using a Student's t-test or a paired t-test. One-way or two-way ANOVA was performed when appropriate. For the post hoc test in the ANOVA, a Tukey's multiple-comparison test was performed. Categorical data were compared with Fisher's exact test. Differences with P values of <0.05 were considered significant. Statistical analyses were conducted with Graph Pad Prism version 6. The APD restitution curves were constructed with Origin 5.0 (Microcal Co., Northampton, MA, USA).

3. Results

3.1. Animal characteristics

The heart weight / body weight ratio in SHR was greater compared with that in WKY rats (heart weight / body weight ratio: 4.70 ± 0.13 mg/g in WKY rats vs. 6.61 ± 0.12 mg/g in SHRs, $P < 0.0001$, n=12).

3.2. Dose–response relation for calcium transient amplitude by isoproterenol in WKY and SHR groups

To assess the β- adrenoreceptor responsiveness, we evaluated dose-response relationship for calcium transient (CaT) amplitude by isoproterenol in WKY rats and SHRs. Each heart was perfused with increasing doses of isoproterenol: 1, 30, 100, 300 nM, and 1 μM. There was no significant difference in the half maximal effective concentration (EC_{50}) value between the two groups (WKY: 60.1 ± 4.28 nM, SHR: 63.9 ±8.58 nM, both n = 3, P = 0.71). The maximal stimulatory effect (E_{max}) by isoproterenol as a function of baseline CaT amplitude was not different between the two groups (WKY: 120 ± 11.3 %, SHR: 146 ± 30.5 %, both n = 3, P =0.46).

3.3. Incidence of sustained ventricular arrhythmias in WKY and SHR groups

To elucidate the effects of apamin on arrhythmogenesis induced by β-adrenoreceptor stimulation, we studied the inducibility of sustained ventricular arrhythmias (SVAs) by burst pacing in WKY and SHR groups (Fig. 1). In a WKY rat, the SVA was not induced during baseline, isoproterenol (100 nM) perfusion and isoproterenol plus apamin (100 nM) perfusion (Fig. 1A). On the other hand, in a SHR, the SVA was induced during isoproterenol perfusion, but it was prevented by apamin

(Fig. 1C). In summary, the incidence of SVAs was not significantly changed in the WKY group (0% in control [n = 5], 0% in the presence of isoproterenol [n = 5] and 20% in isoproterenol plus apamin [n = 5]). (Fig. 1B). While, in the SHR group, the incidence of SVAs was significantly increased in the presence of isoproterenol and it was suppressed by apamin perfusion (0% in control [n = 5], 71% in the presence of isoproterenol [n = 7] and 0% in isoproterenol plus apamin [n = 7]) (Fig. 1D).

3.4. Effects of β-adrenoreceptor stimulation in the absence or presence of apamin on action potentials and calcium transients in WKY and SHR groups

Fig. 2A and 2C show representative action potential (*left* panel) and CaT (*right* panel) tracings from the epicardial surface of left ventricular anterior wall in a WKY rat and an SHR, respectively. Amplitude of the action potential and CaT is normalized to recognize their duration (APD_{90} and $CaTD_{90}$) clearly. Fig. 2B shows representative APD_{90} maps and $CaTD_{90}$ maps in a WKY rat. The APD_{90} in a WKY rat was shortened by isoproterenol and it was not affected by apamin in the presence of isoproterenol (100.3 ± 3.84 ms in control [n = 7], 91.8 ± 2.70 ms in the presence of isoproterenol [n = 7], P = 0.03 vs. control; 93.3 ± 2.83 ms in the presence of isoproterenol plus apamin [n = 7], P = 0.83 vs. isoproterenol) (Fig. 3A). Similarly, $CaTD_{90}$ was shortened by

isoproterenol and apamin did not change the isoproterenol-induced $CaTD_{90}$ shortening (133.3 ± 1.6 ms in control [n = 7], 114.4 ± 4.4 ms in the presence of isoproterenol [n = 7], *P* = 0.01 vs. control, 115.0 ± 2.7 ms in the presence of isoproterenol plus apamin [n = 7], *P* = 0.89 vs. isoproterenol) (Fig. 3B). On the other hand, in the SHR group, APD_{90} was abbreviated by isoproterenol and this abbreviation of APD_{90} was partially reversed by apamin (134.4 ± 5.50 ms in control [n = 10], 116.6 ± 5.05 ms in the presence of isoproterenol [n = 10], *P* = 0.0007 vs. control, 125.4 ± 3.80 ms in the presence of isoproterenol plus apamin [n = 10], *P* = 0.011 vs. isoproterenol) (Figs. 2C, 2D and Fig 3D). In contrast, $CaTD_{90}$ in the SHR group showed a response similar to that in the WKY group (140.6 ± 5.21 ms in control [n = 10], 117.5 ± 4.31 ms in the presence of isoproterenol [n = 10], *P* = 0.0005 vs. control, 118.6 ± 3.66 ms in the presence of isoproterenol plus apamin [n = 10], *P* = 0.94 vs. isoproterenol) (Figs. 2C, 2D and Fig. 3E). The rise time of CaT was calculated as the time required for fluorescence to change from 10% to 90% of peak waveform (Laurita and Singal, 2001). In both WKY and SHR groups, the rise time was shortened by isoproterenol administration, which was not significantly changed when apamin was perfused in the presence of isoproterenol (WKY group: 11.2 ± 0.14 ms in control [n = 7], 9.65 ± 0.41 ms in the presence of isoproterenol [n = 7], P < 0.0001 vs. control, 10.1 ± 0.33 ms in the presence of

isoproterenol plus apamin [n = 7], P = 0.37 vs. isoproterenol; SHR group: 16.0 ± 1.45 ms in control [n = 10], 12.4 ± 1.11 ms in the presence of isoproterenol [n = 10], P = 0.0007 vs. control, 13.8 ± 1.4 ms in the presence of isoproterenol plus apamin [n = 10], P=0.11 vs. isoproterenol) (Figs. 3C and 3F).

3.5. APD restitution curve

Representative APD restitution curves for the WKY and SHR groups are shown in Figs. 4A and 4C, and the maximal slope of APD restitution curve for each group is summarized in Figs. 4B and 4D, respectively. The maximal slope was not significantly changed in the WKY group (0.43 ± 0.08 in control [n = 4], 0.50 ± 0.05 in the presence of isoproterenol [n = 4], 0.46 ± 0.07 in the presence of isoproterenol plus apamin [n = 4]) (Figure 4B). However, in the SHR group, it was increased by isoproterenol administration and was decreased in the presence of apamin. On the other hand, neither 4-AP (1 mM) nor E-4031 (1 μ M) significantly reduced the maximal slope of APD restitution (0.42 ± 0.05 in control [n = 4], 1.57 ± 0.3 in the presence of isoproterenol [n = 5], *P* = 0.01 vs. control; 0.44 ± 0.15 in the presence of isoproterenol plus apamin [n = 4], *P* = 0.02 vs. isoproterenol; 0.91 ± 0.18 in the presence of isoproterenol plus 4 – AP [n = 3], *P* = 0.66 vs. isoproterenol; 1.07 ± 0.23 in the presence

of isoproterenol plus E – 4031 [n = 3], *P* = 0.50 vs. isoproterenol) (Fig. 4D).

3.6. CaMKII activity

Figs. 5A and 5B show the CaMKII activity at baseline and in the presence of isoproterenol (100 nM) in both WKY and SHR groups. We evaluated the CaMKII activity of the LV tissue from isolated perfused hearts at a pacing cycle length of 180 ms. At baseline, tissue CaMKII activity in 3 hearts from WKY rats averaged 33.5 ± 2.9 % of the maximal CaMKII activity which was determined by adding saturating Ca^{2+} and calmodulin to the same tissue sample. During isoproterenol (100 nM) perfusion, CaMKII activity in 3 hearts averaged 36.0 ± 1.0 % of the maximum in the WKY group (Fig. 5A, P = 0.47 vs. control). While, in the SHR group, at baseline, CaMKII activity in 3 hearts averaged 40.3 ± 1.3 % of the maximum. During isoproterenol (100 nM) perfusion, CaMKII activity significantly increased to 46.1 ± 0.9 % of the maximum (Fig. 5B, P = 0.02 vs. control).

3.7. Effects of CaMKII inhibition and apamin on action potential and calcium transient changes produced by β-adrenoreceptor stimulation in SHRs

Fig. 6A shows representative action potential waveforms and APD_{90} maps of a

SHR in the presence of isoproterenol plus KN93 (1 μM), an inhibitor of CaMKII, before and after apamin perfusion. APD_{90} was not significantly changed when apamin was added in the presence of isoproterenol plus KN93 (110.0 ± 2.6 ms in in the presence of isoproterenol plus KN93, [n = 8], 110.8 ± 2.2 ms in in the presence of isoproterenol, KN93 plus apamin, [n = 8], P = 0.68 vs. isoproterenol plus KN93) (Fig. 6B). Representative CaT waveforms and $CaTD_{90}$ maps in the presence of isoproterenol plus KN93 before and after apamin perfusion are shown in Fig. 6C. Similarly, apamin did not change $CaTD_{90}$ and rise time of CaT (not shown) under the condition of CaMKII inhibition (111.4 ± 3.2 ms in the presence of isoproterenol plus KN93, [n = 8], 111.7 ± 2.3 ms in the presence of isoproterenol, KN93 plus apamin, [n = 8], P = 0.88 vs. isoproterenol plus KN93) (Fig 6D).

4. Discussion

In the present study, we have demonstrated that SK channel currents contribute to electrophysiological changes and susceptibility to SVAs under β-adrenoreceptor stimulation in a rat model of cardiac hypertrophy. During β- adrenoreceptor stimulation, the maximal slope of APD restitution curve in hypertrophied hearts was steepened, and it was flattened by apamin, a blocker of SK channel currents. In addition, CaMKII

activity was elevated by isoproterenol perfusion especially in hypertrophied myocardium, and KN-93, a pharmacological inhibitor of CaMKII, abolished the prolongation of APD by apamin under β- adrenoreceptor stimulation.

Previous reports showed that APD was abbreviated by β- adrenoreceptor stimulation in normal rabbit (Hoeker et al., 2014) and failing human hearts (Lang et al., 2015). However, the mechanisms of APD shortening during β- adrenoreceptor stimulation is not completely elucidated. Cardiac K^+ channels responsible for action potential repolarization were regulated by β-adrenoreceptor stimulation (Harmati et al., 2011; Volders et al., 2003; Zhu et al., 2013). In this report, APD was abbreviated by β-adrenoreceptor stimulation in both WKY rats and SHRs (Figs. 2A and 2B), and the APD in SHRs was specifically prolonged by apamin under β- adrenoreceptor stimulation. Therefore, SK channel activation could be associated with abbreviation of APD under β- adrenoreceptor stimulation in SHRs.

The present study confirmed a previous observation that the relative increase in CaT with the addition of isoproterenol was similar between WKY rats and SHRs (Bing et al., 1991). That is, there was no significant difference in the E_{max} and EC_{50} of CaT amplitude by isoproterenol between the two groups. Additionally, we simultaneously mapped action potentials and CaTs during β- adrenoreceptor stimulation. CaT duration

was significantly abbreviated and its rise time became faster by β- adrenoreceptor stimulation, as compared with those during baseline. Neither CaT duration nor the rise time of CaT was affected by apamin under β- adrenoreceptor stimulation in both WKY rats and SHRs. Based on these findings, the mechanism of SK channel activation under β- adrenoreceptor stimulation in SHRs could not be explained by alteration of the intracellular calcium handling.

CaMKII is recognized as one of the important targets in β-adrenoreceptor signaling (Yoo et al., 2009), and is upregulated in hypertrophied and failing myocardium from animal models (Anderson et al., 2011). With regard to ion channel regulation, adenovirus transfer of CaMKIIδ increased K^+ currents within 24 hours in rabbit ventricular myocytes, and some components of these currents were reduced by AIP (a CaMKII inhibitor), suggesting CaMKII acutely increases certain K^+ currents (Wagner et al., 2009). Consistently, we demonstrated (a) significant increase in the CaMKII activity in response to isoproterenol (100 nM) perfusion especially in SHRs (Fig. 5) and (b) KN93 (a CaMKII inhibitor) inhibition of the apamin-sensitive component of APD under β- adrenoreceptor stimulation in SHRs (Fig. 6). These findings suggest that β-adrenoreceptor stimulation activates SK channels through the CaMKII-dependent mechanism.

A steep APD restitution slope can contribute to breakup of reentrant waves into cardiac fibrillation (Weiss et al., 2000). Consistent with this idea, β- adrenoreceptor stimulation increased the incidence of SVAs and maximum slope of APD restitution specifically in SHRs, both of which were suppressed by apamin. We also evaluated a role of other potassium channels using 4-AP and E-4031, a blocker of I_{to} and I_{Kr}, respectively, on the APD restitution slope. In contrast to apamin, it was only slightly (but not significantly) reduced by 4- AP and E-4031. Little effect of 4-AP at the shorter DIs (less than 50 ms in Fig. 4C) would be attributable to decrease in I_{to} by high-frequency stimulation (Wettwer et al., 1993), thereby resulting in only a small reduction of the maximum slope. Similarly, E-4031 could not effectively reduce the steepness of APD restitution due to the reverse use dependent property of class III antiarrhythmic agents as well as low density of I_{Kr} in rat ventricular myocytes (Hondeghem and Snyders, 1990; Matsuda et al., 2005; Pond et al., 2000). Taken together, β-adrenoreceptor stimulation could steepen the maximal slope of APD restitution curve via activation of SK channels specifically in cardiac hypertrophy, which promotes the occurrence and maintenance of SVAs.

SK channels are expressed in the vascular endothelium and smooth muscle of the heart, thereby regulating coronary flow. Actually, it was reported that apamin

suppressed coronary artery flow in rat hearts (Mishra et al., 2013). Therefore, we should interpret the present findings with great caution in terms of the effects of apamin on other tissues. The choice of anaesthetic in animal arrhythmia studies is an important issue, because some anaesthetics affect occurrence of arrhythmias (Curtis et al., 2013). With regard to the mixture of medetomidine, midazolam, and butorphanol (Kirihara et al., 2016) , there are no studies showing that this method is neutral for heart rhythm in rats.

5. Conclusions

In cardiac hypertrophy, β- adrenoreceptor simulation steepens the maximal slope of APD restitution curve and unmasks susceptibility to SVAs by programed electrical stimulations. This arrhythmogenic β- adrenoreceptor signaling appears to be mediated through activation of SK channels via the CaMKII-dependent pathway.

Acknowledgments

We thank N. Ikeda, Yamane M and Y. Kimura for technical assistance in the experiments.

Conflicts of interest

No conflicts of interest, financial or otherwise, are declared by the author (s).

Reference

Adelman, J.P., Maylie, J., Sah, P., 2012. Small-conductance Ca2+-activated K+ channels: form and function. Annu Rev Physiol 74, 245-269.

Anderson, M.E., Brown, J.H., Bers, D.M., 2011. CaMKII in myocardial hypertrophy and heart failure. J Mol Cell Cardiol 51, 468-473.

Bing, O.H., Brooks, W.W., Conrad, C.H., Sen, S., Perreault, C.L., Morgan, J.P., 1991. Intracellular calcium transients in myocardium from spontaneously hypertensive rats during the transition to heart failure. Circ Res 68, 1390-1400.

Chan, V., Fenning, A., Levick, S.P., Loch, D., Chunduri, P., Iyer, A., Teo, Y.L., Hoey, A., Wilson, K., Burstow, D., Brown, L., 2011. Cardiovascular changes during maturation and ageing in male and female spontaneously hypertensive rats. J Cardiovasc Pharmacol 57, 469-478.

Chang, P.C., Hsieh, Y.C., Hsueh, C.H., Weiss, J.N., Lin, S.F., Chen, P.S., 2013. Apamin induces early afterdepolarizations and torsades de pointes ventricular arrhythmia from failing rabbit ventricles exhibiting secondary rises in intracellular calcium. Heart Rhythm 10, 1516-1524.

Chua, S.K., Chang, P.C., Maruyama, M., Turker, I., Shinohara, T., Shen, M.J., Chen, Z., Shen, C., Rubart-von der Lohe, M., Lopshire, J.C., Ogawa, M., Weiss, J.N., Lin, S.F., Ai, T., Chen, P.S., 2011. Small-conductance calcium-activated potassium channel and recurrent ventricular fibrillation in failing rabbit ventricles. Circ Res 108, 971-979.

Curran, J., Hinton, M.J., Rios, E., Bers, D.M., Shannon, T.R., 2007. Beta-adrenergic enhancement of sarcoplasmic reticulum calcium leak in cardiac myocytes is mediated by calcium/calmodulin-dependent protein kinase. Circ Res 100, 391-398.

Curtis, M.J., Hancox, J.C., Farkas, A., Wainwright, C.L., Stables, C.L., Saint, D.A., Clements-Jewery, H., Lambiase, P.D., Billman, G.E., Janse, M.J., Pugsley, M.K., Ng, G.A., Roden, D.M., Camm, A.J., Walker, M.J., 2013. The Lambeth Conventions (II): guidelines for the study of animal and human ventricular and supraventricular arrhythmias. Pharmacol Ther 139, 213-248.

Goldhaber, J.I., Xie, L.H., Duong, T., Motter, C., Khuu, K., Weiss, J.N., 2005. Action potential duration restitution and alternans in rabbit ventricular myocytes: the key role of intracellular calcium cycling. Circ Res 96, 459-466.

Han, J., Garciadejalon, P., Moe, G.K., 1964. ADRENERGIC EFFECTS ON VENTRICULAR

VULNERABILITY. Circ Res 14, 516-524.

Harmati, G., Banyasz, T., Barandi, L., Szentandrassy, N., Horvath, B., Szabo, G., Szentmiklosi, J.A., Szenasi, G., Nanasi, P.P., Magyar, J., 2011. Effects of beta-adrenoceptor stimulation on delayed rectifier K(+) currents in canine ventricular cardiomyocytes. Br J Pharmacol 162, 890-896.

Hoeker, G.S., Hood, A.R., Katra, R.P., Poelzing, S., Pogwizd, S.M., 2014. Sex differences in beta-adrenergic responsiveness of action potentials and intracellular calcium handling in isolated rabbit hearts. PLoS One 9, e111411.

Hondeghem, L.M., Snyders, D.J., 1990. Class III antiarrhythmic agents have a lot of potential but a long way to go. Reduced effectiveness and dangers of reverse use dependence. Circulation 81, 686-690.

Kirihara, Y., Takechi, M., Kurosaki, K., Kobayashi, Y., Saito, Y., Takeuchi, T., 2016. Effects of an anesthetic mixture of medetomidine, midazolam, and butorphanol in rats-strain difference and antagonism by atipamezole. Exp Anim 65, 27-36.

Kohya, T., Yokoshiki, H., Tohse, N., Kanno, M., Nakaya, H., Saito, H., Kitabatake, A., 1995. Regression of left ventricular hypertrophy prevents ischemia-induced lethal arrhythmias. Beneficial effect of angiotensin II blockade. Circ Res 76, 892-899.

Lang, D., Holzem, K., Kang, C., Xiao, M., Hwang, H.J., Ewald, G.A., Yamada, K.A., Efimov, I.R., 2015. Arrhythmogenic remodeling of beta2 versus beta1 adrenergic signaling in the human failing heart. Circ Arrhythm Electrophysiol 8, 409-419.

Laurita, K.R., Singal, A., 2001. Mapping action potentials and calcium transients simultaneously from the intact heart. Am J Physiol Heart Circ Physiol 280, H2053-2060.

Litovsky, S.H., Antzelevitch, C., 1990. Differences in the electrophysiological response of canine ventricular subendocardium and subepicardium to acetylcholine and isoproterenol. A direct effect of acetylcholine in ventricular myocardium. Circ Res 67, 615-627.

Maruyama, M., Joung, B., Tang, L., Shinohara, T., On, Y.K., Han, S., Choi, E.K., Kim, D.H., Shen, M.J., Weiss, J.N., Lin, S.F., Chen, P.S., 2010. Diastolic intracellular calcium-membrane voltage coupling gain and postshock arrhythmias: role of purkinje fibers and triggered activity. Circ Res 106, 399-408.

Matsuda, T., Takeda, K., Ito, M., Yamagishi, R., Tamura, M., Nakamura, H., Tsuruoka, N., Saito, T., Masumiya, H., Suzuki, T., Iida-Tanaka, N., Itokawa-Matsuda, M., Yamashita, T., Tsuruzoe, N., Tanaka, H., Shigenobu, K., 2005. Atria selective prolongation by NIP-142, an antiarrhythmic agent, of refractory period and action potential duration in guinea pig myocardium. J Pharmacol Sci 98, 33-40.

Meredith, I.T., Broughton, A., Jennings, G.L., Esler, M.D., 1991. Evidence of a selective increase in cardiac sympathetic activity in patients with sustained ventricular arrhythmias. N Engl J Med 325, 618-624.

Mishra, R.C., Belke, D., Wulff, H., Braun, A.P., 2013. SKA-31, a novel activator of SK(Ca) and IK(Ca) channels, increases coronary flow in male and female rat hearts. Cardiovasc Res 97, 339-348.

Mitsuyama, H., Yokoshiki, H., Watanabe, M., Mizukami, K., Shimokawa, J., Tsutsui, H., 2014.

Ca2+/calmodulin-dependent protein kinase II increases the susceptibility to the arrhythmogenic action potential alternans in spontaneously hypertensive rats. Am J Physiol Heart Circ Physiol 307, H199-206.

Mizukami, K., Yokoshiki, H., Mitsuyama, H., Watanabe, M., Tenma, T., Takada, S., Tsutsui, H., 2015. Small-conductance Ca2+-activated K+ current is upregulated via the phosphorylation of CaMKII in cardiac hypertrophy from spontaneously hypertensive rats. Am J Physiol Heart Circ Physiol 309, H1066-1074.

Nagy, N., Szuts, V., Horvath, Z., Seprenyi, G., Farkas, A.S., Acsai, K., Prorok, J., Bitay, M., Kun, A., Pataricza, J., Papp, J.G., Nanasi, P.P., Varro, A., Toth, A., 2009. Does small-conductance calcium-activated potassium channel contribute to cardiac repolarization? J Mol Cell Cardiol 47, 656-663.

Pezhouman, A., Singh, N., Song, Z., Nivala, M., Eskandari, A., Cao, H., Bapat, A., Ko, C.Y., Nguyen, T., Qu, Z., Karagueuzian, H.S., Weiss, J.N., 2015. Molecular Basis of Hypokalemia-Induced Ventricular Fibrillation. Circulation 132, 1528-1537.

Pond, A.L., Scheve, B.K., Benedict, A.T., Petrecca, K., Van Wagoner, D.R., Shrier, A., Nerbonne, J.M., 2000. Expression of distinct ERG proteins in rat, mouse, and human heart. Relation to functional I(Kr) channels. J Biol Chem 275, 5997-6006.

Volders, P.G., Stengl, M., van Opstal, J.M., Gerlach, U., Spatjens, R.L., Beekman, J.D., Sipido, K.R., Vos, M.A., 2003. Probing the contribution of IKs to canine ventricular repolarization: key role for beta-adrenergic receptor stimulation. Circulation 107, 2753-2760.

Wagner, S., Hacker, E., Grandi, E., Weber, S.L., Dybkova, N., Sossalla, S., Sowa, T., Fabritz, L., Kirchhof, P., Bers, D.M., Maier, L.S., 2009. Ca/calmodulin kinase II differentially modulates potassium currents. Circ Arrhythm Electrophysiol 2, 285-294.

Weiss, J.N., Chen, P.S., Qu, Z., Karagueuzian, H.S., Garfinkel, A., 2000. Ventricular fibrillation: how do we stop the waves from breaking? Circ Res 87, 1103-1107.

Wettwer, E., Amos, G., Gath, J., Zerkowski, H.R., Reidemeister, J.C., Ravens, U., 1993. Transient outward current in human and rat ventricular myocytes. Cardiovasc Res 27, 1662-1669.

Yoo, B., Lemaire, A., Mangmool, S., Wolf, M.J., Curcio, A., Mao, L., Rockman, H.A., 2009. Beta1-adrenergic receptors stimulate cardiac contractility and CaMKII activation in vivo and enhance cardiac dysfunction following myocardial infarction. Am J Physiol Heart Circ Physiol 297, H1377-1386.

Zhu, Y., Ai, X., Oster, R.A., Bers, D.M., Pogwizd, S.M., 2013. Sex differences in repolarization and slow delayed rectifier potassium current and their regulation by sympathetic stimulation in rabbits. Pflugers Arch 465, 805-818.

Figure Legends

Fig. 1. Incidence of sustained ventricular arrhythmias under β-adrenoreceptor stimulation.

A: Representative electrogram traces obtained from WKY rats. An electrogram trace in control, under isoproterenol (100nM) perfusion, and in the presence of isoproterenol plus apamin (100nM) was shown, respectively.

B: The sum of sustained ventricular arrhythmias (SVAs) incidences in the WKY group. Control, n=5; isoproterenol, n=5; isoproterenol plus apamin, n=5

C: Representative electrogram traces obtained from SHRs. The upper panel shows an electrogram trace in control and the middle panel illustrates an electrogram trace by burst pacing under isoproterenol (100nM) administration. The bottom panel shows an electrogram trace in the presence of isoproterenol plus apamin (100nM).

D: The sum of SVAs incidence in the SHR group $^{*}P < 0.05$ vs. Control, † $P < 0.05$ vs. in the presence of isoproterenol plus apamin (Fisher's exact test).

Control, n=5; isoproterenol, n=7; isoproterenol plus apamin, n=7

WKY: Wistar-Kyoto; SHR: Spontaneous Hypertensive rat; ISO: isoproterenol

Fig. 2. Effects of β-adrenoreceptor stimulation by isoproterenol in the absence or presence of apamin on action potentials and calcium transients in a WKY rat and an SHR.

A: Representative optical membrane potential tracings (*left panel*) and calcium transient tracings (*right panel*) in control, isoproterenol (100nM), and isoproterenol plus apamin (100nM), respectively.

B: The representative changes in APD_{90} (*top*) and $CaTD_{90}$ (*bottom*) maps.

C: Representative optical membrane potential tracings (*left panel*) and calcium transient tracings (*right panel*) in control, isoproterenol (100nM), and isoproterenol plus apamin (100nM), respectively.

D: The representative changes in APD_{90} (*top*) and $CaTD_{90}$ (*bottom*) maps.

APD_{90}: action potential duration measured at 90% repolarization; $CaTD_{90}$: calcium transient duration measured at 90% recovery

Fig. 3. Summary of effects of isoproterenol and apamin on the optical APD_{90} and $CaTD_{90}$ in both the WKY and SHR groups.

Each graph shows APD_{90} (A, D), $CaTD_{90}$ (B, E) and rise time of CaT (C, F) in control,

isoproterenol administration and isoproterenol plus apamin added in WKY rats (A, B, C) (n=7) and SHRs (D, E, F) (n=10), respectively. *$P < 0.05$: vs. Control, †$P < 0.05$: vs. isoproterenol (One-way repeated ANOVA post hoc Tukey's multiple-comparison test). CaT: calcium transient. Other abbreviations are given in Fig.2.

Fig. 4. APD restitution curves in the WKY and SHR groups.

APD restitution curves in a WKY rat (A) and in an SHR (C) are given. The maximum slope of APD restitution curves are summarized for the WKY group (B) (n=4) and SHR group (D) (control, isoproterenol plus apamin: n=4, isoproterenol: n=5, 4-AP, E-4031: n=3). *$P < 0.05$: vs. Control, †$P < 0.05$: vs. isoproterenol (One-way ANOVA post hoc Tukey's multiple-comparison test).

APD_{90}: action potential duration measured at 90% repolarization; DI: diastolic interval; ISO: isoproterenol; 4-AP: pyridine-4-amine; E-4031: N-[4-[1-[2-(6-methylpyridin-2-yl)ethyl]piperidine-4-carbonyl]phenyl]methanesulfonamide

Fig. 5. CaMKII activity in the absence and presence of isoproterenol.

CaMKII activity in control and in the presence of isoproterenol for the WKY group (A)

and SHR group (B) (Control, isoproterenol n=3 for each condition). *$P < 0.05$ vs. Control (Student's t-test).

Fig. 6. Pharmacological inhibition of CaMKII by KN93 prevents the apamin actions on the APD_{90} and $CaTD_{90}$ of SHRs under β- adrenoreceptor stimulation.

A: Representative optical action potentials (*left*) and the APD_{90} map (*right*) of LV from an SHR in the presence of KN93 (1 μM), an inhibitor of CaMKII, are given.

B: This graph summarizes the APD_{90} before and after addition of apamin in the presence of isoproterenol plus KN93 (isoproterenol plus KN93, isoproterenol plus KN93 and apamin n=8 for each condition).

C: Representative calcium transients (*left*) and the $CaTD_{90}$ map (*right*) of LV from an SHR in the presence of KN93 (1 μM), an inhibitor of CaMKII, are given.

D: This graph summarizes the $CaTD_{90}$ before and after addition of apamin in the presence of isoproterenol plus KN93 (isoproterenol plus KN93, isoproterenol plus KN93 and apamin n=8 for each condition).

Abbreviations are given in Fig.2.

Fig. 1

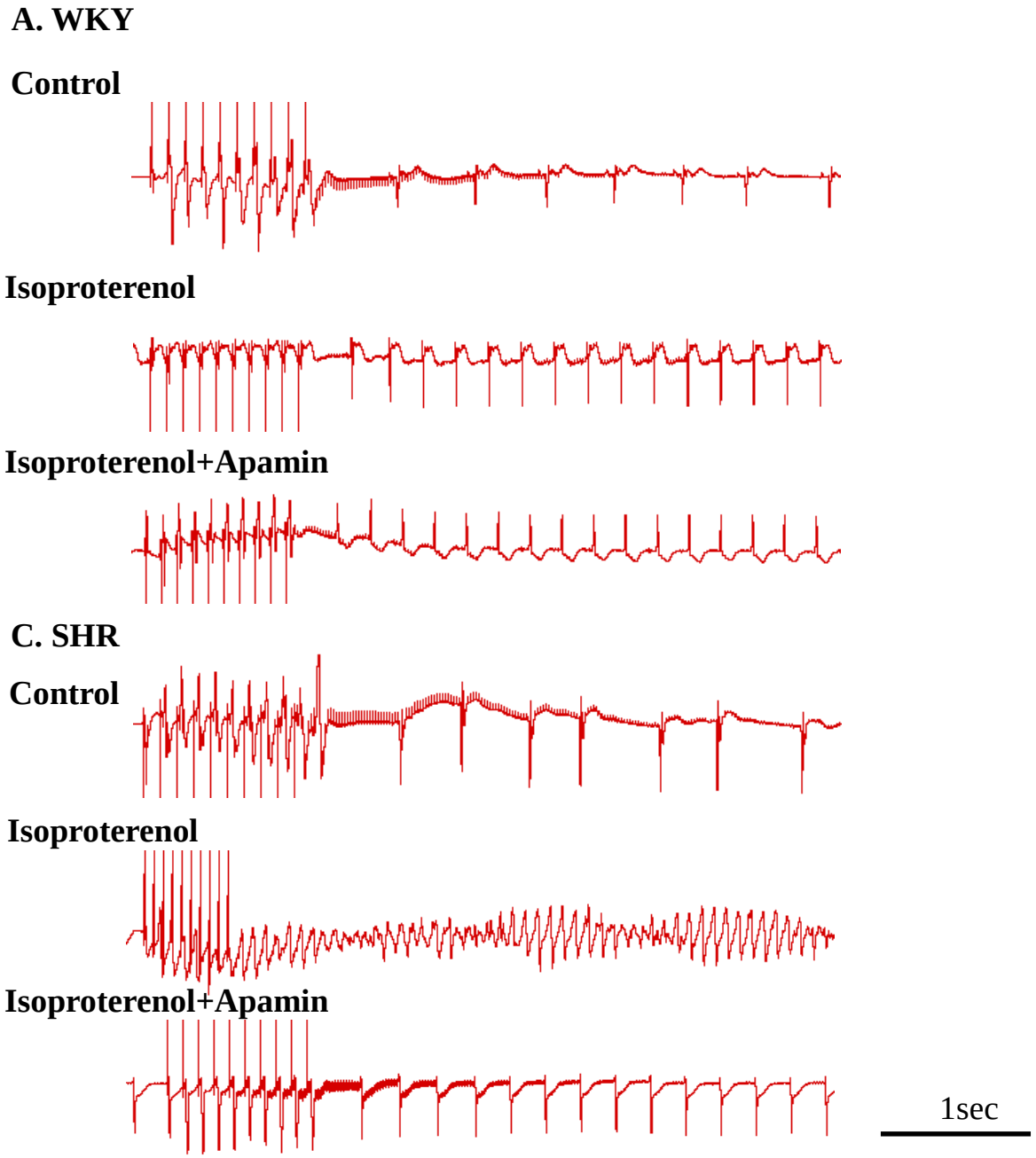
A. WKY
Control
Isoproterenol
Isoproterenol+Apamin
C. SHR
Control
Isoproterenol
Isoproterenol+Apamin
1sec

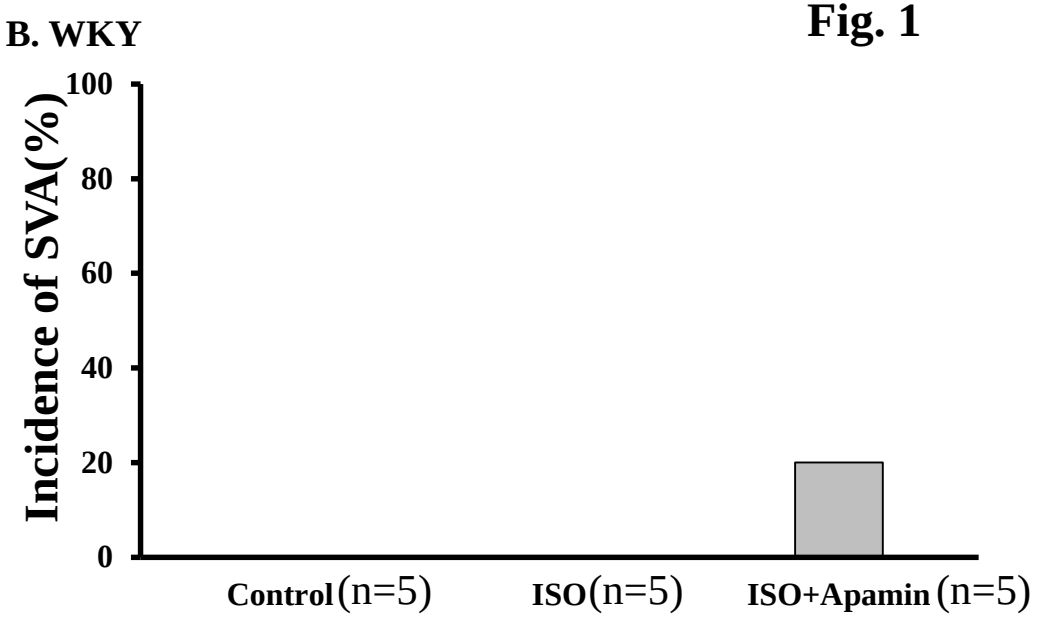
B. WKY
Incidence of SVA(%)
100
80
60
40
20
0
Control (n=5)
ISO (n=5)
ISO+Apamin (n=5)

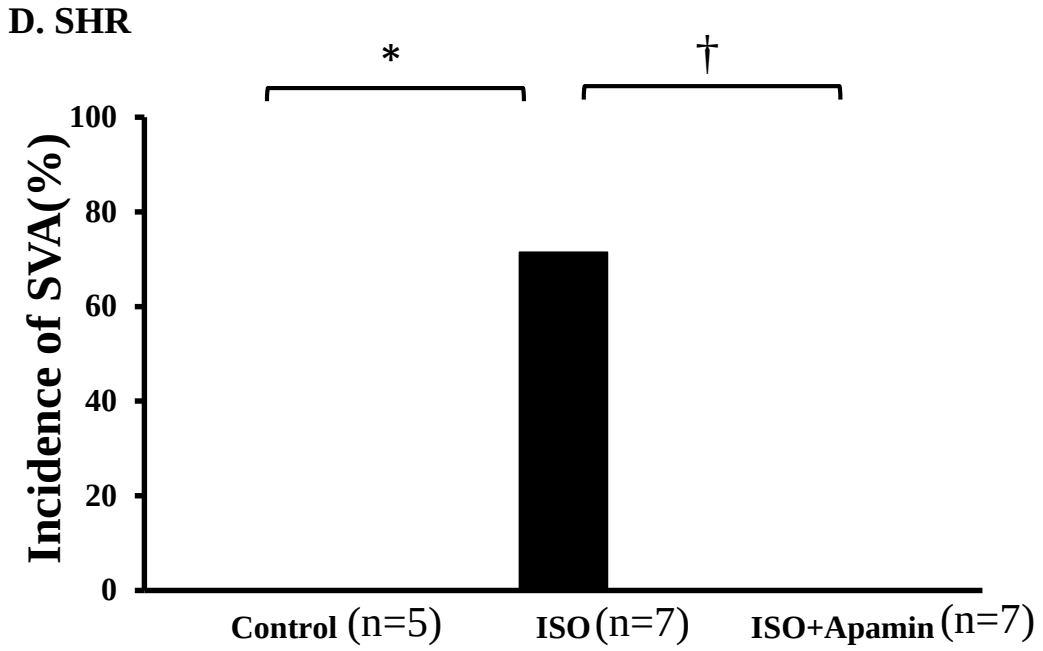
D. SHR
*
†
Incidence of SVA(%)
100
80
60
40
20
0
Control (n=5)
ISO (n=7)
ISO+Apamin (n=7)

Fig. 2

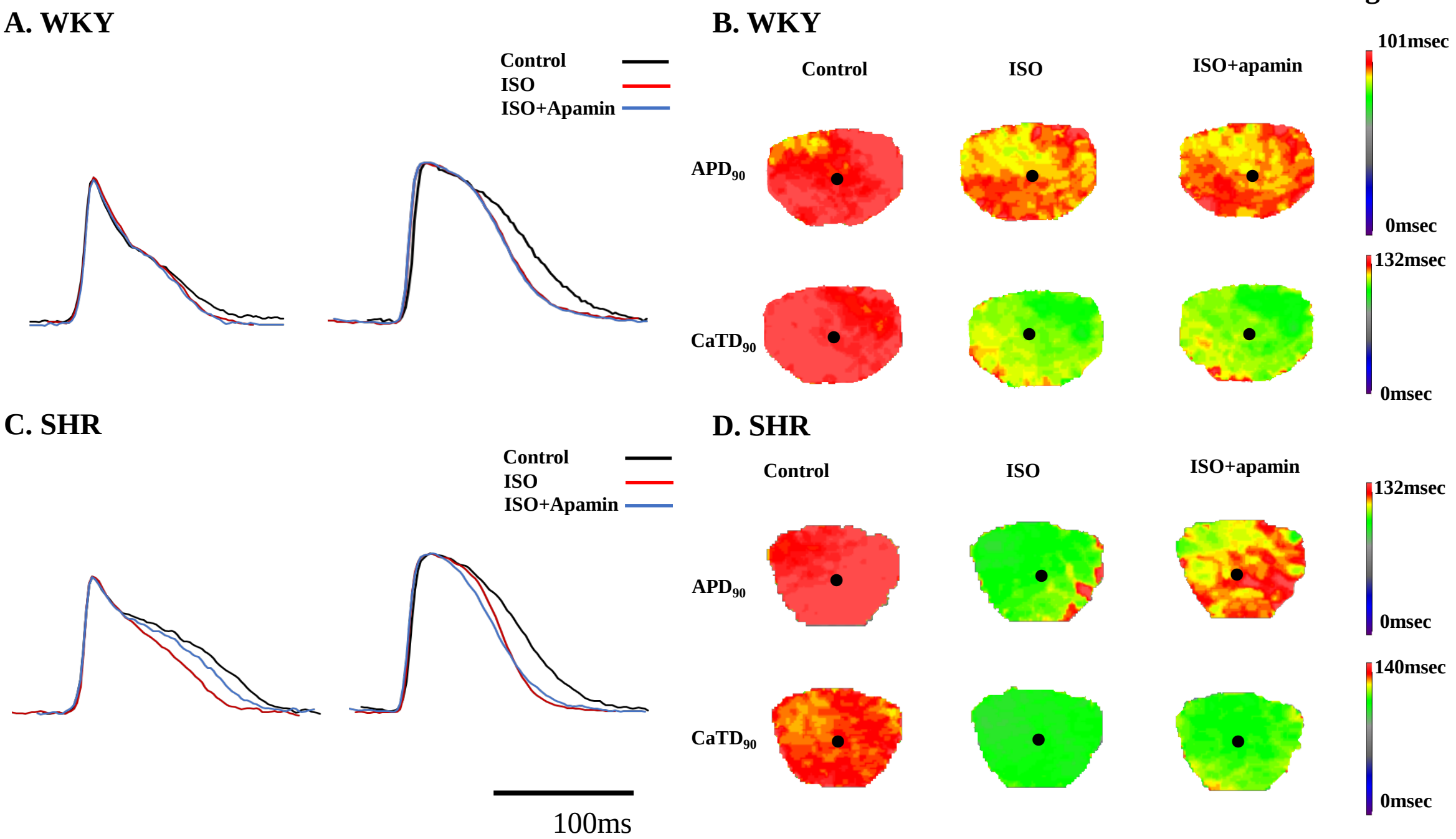
A. WKY
Control
ISO
ISO+Apamin
B. WKY
Control
ISO
ISO+apamin
101msec
0msec
APD90
CaTD90
132msec
0msec
C. SHR
Control
ISO
ISO+Apamin
100ms
D. SHR
Control
ISO
ISO+apamin
132msec
0msec
APD90
CaTD90
140msec
0msec

Fig. 3

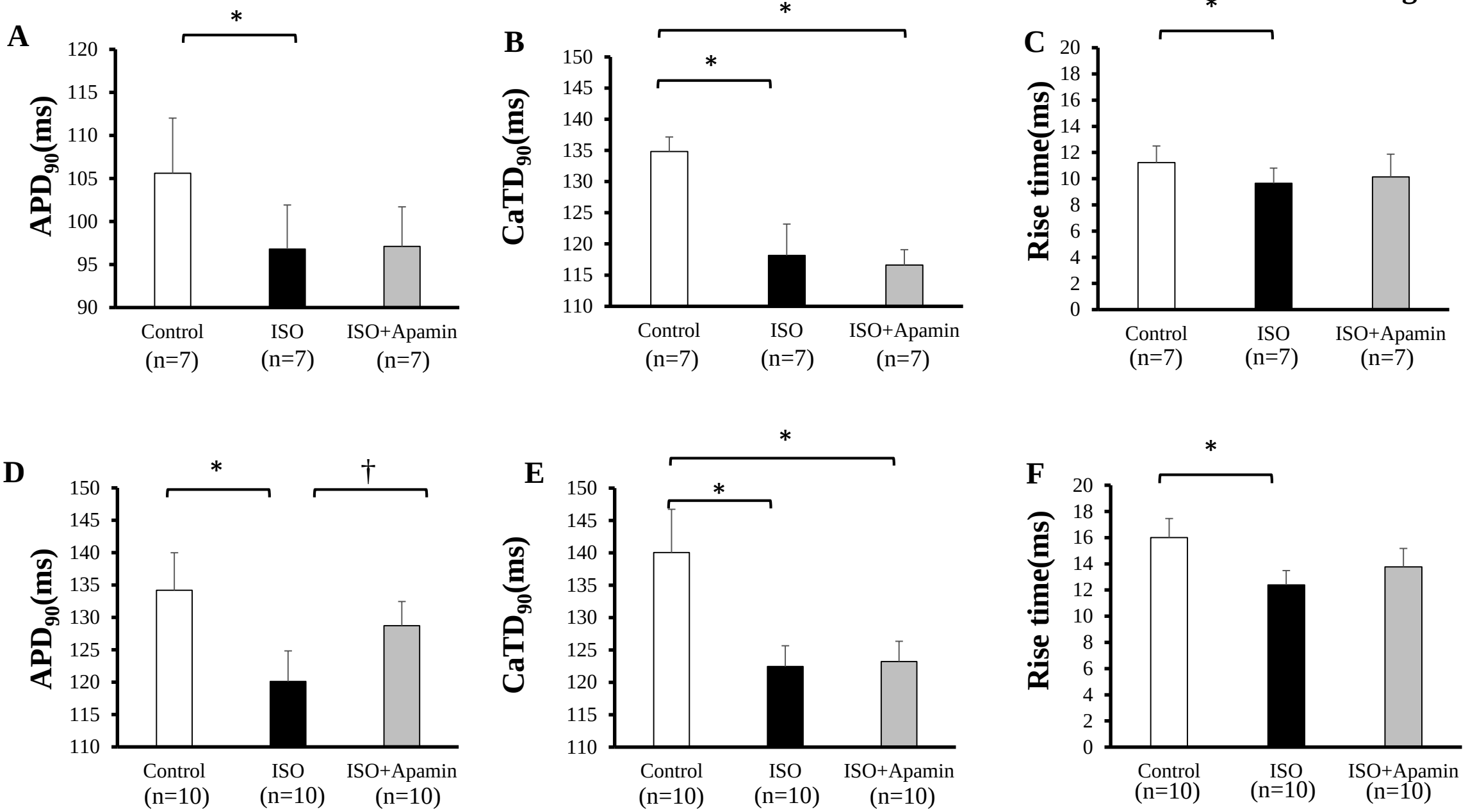
A
B
C
D
E
F
APD90(ms)
CaTD90(ms)
Rise time(ms)
Control
ISO
ISO+Apamin
(n=7)
(n=10)
*
†

Fig. 4

A. WKY

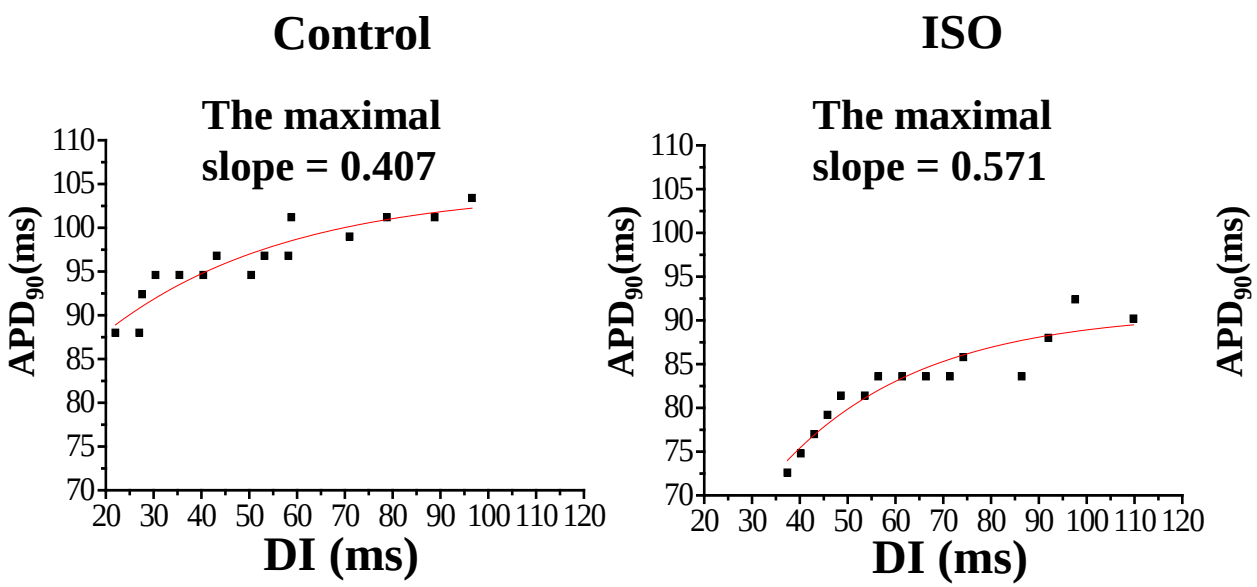

B. WKY

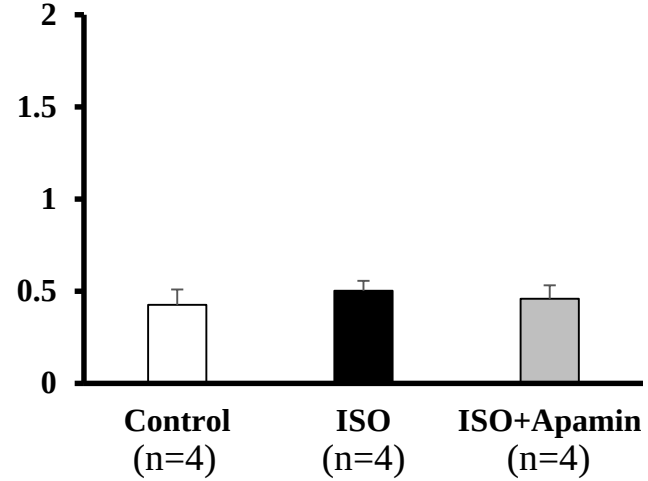

C. SHR

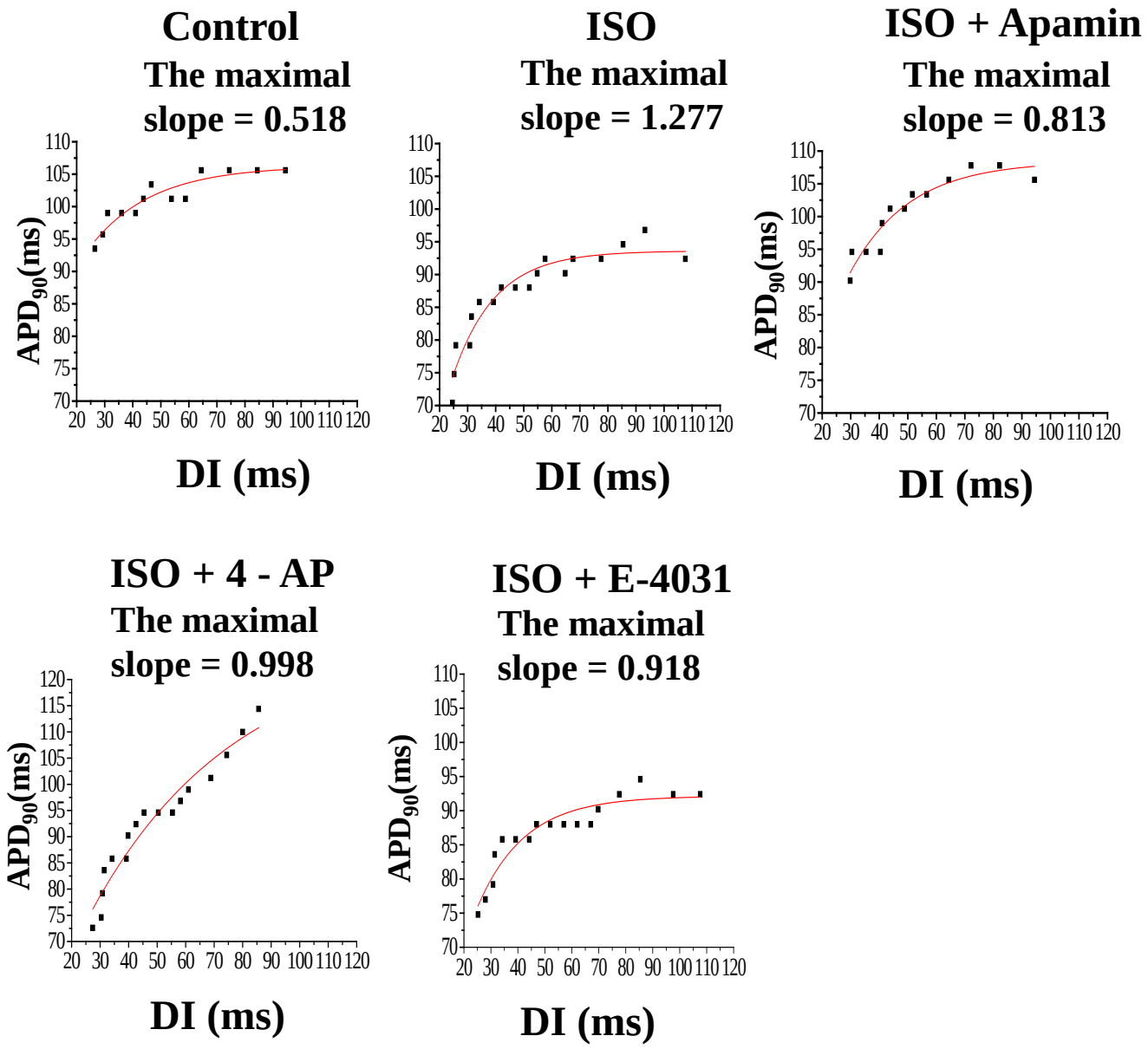
Control
The maximal slope = 0.518
ISO
The maximal slope = 1.277
ISO + Apamin
The maximal slope = 0.813
ISO + 4 - AP
The maximal slope = 0.998
ISO + E-4031
The maximal slope = 0.918
APD90(ms)
DI (ms)

D. SHR

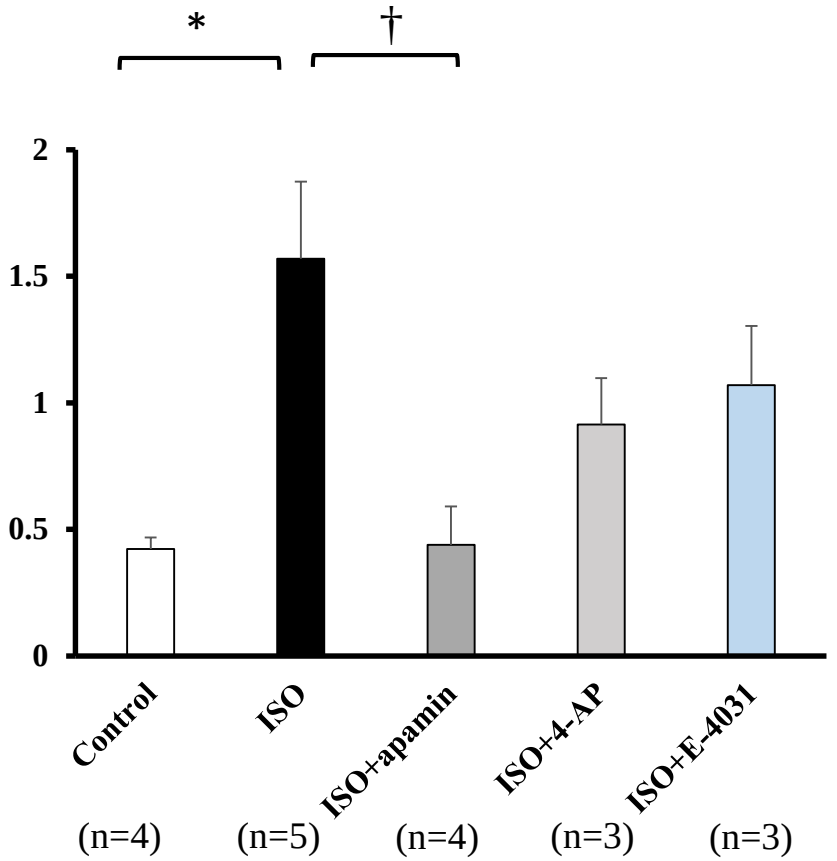
*
†
2
1.5
1
0.5
0
Control
ISO
ISO+apamin
ISO+4-AP
ISO+E-4031
(n=4)
(n=5)
(n=4)
(n=3)
(n=3)

Fig. 5

A. WKY

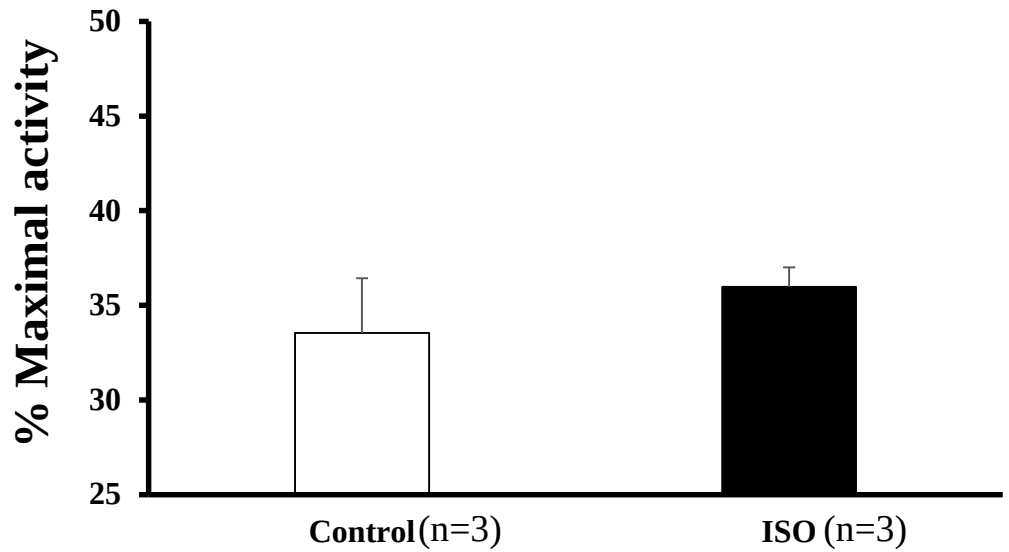

B. SHR

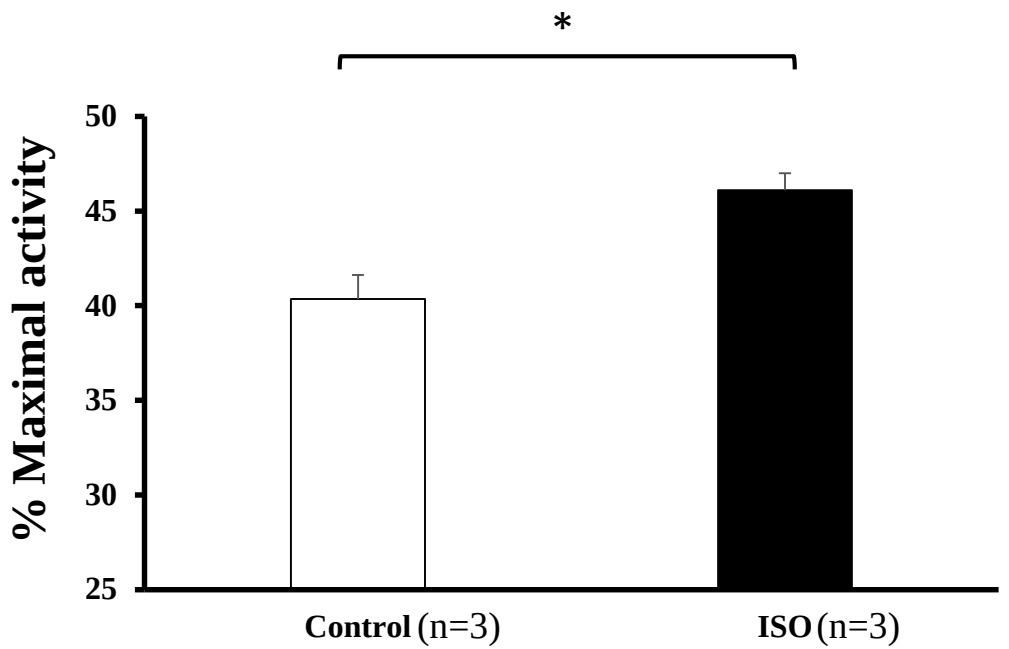

Fig. 6

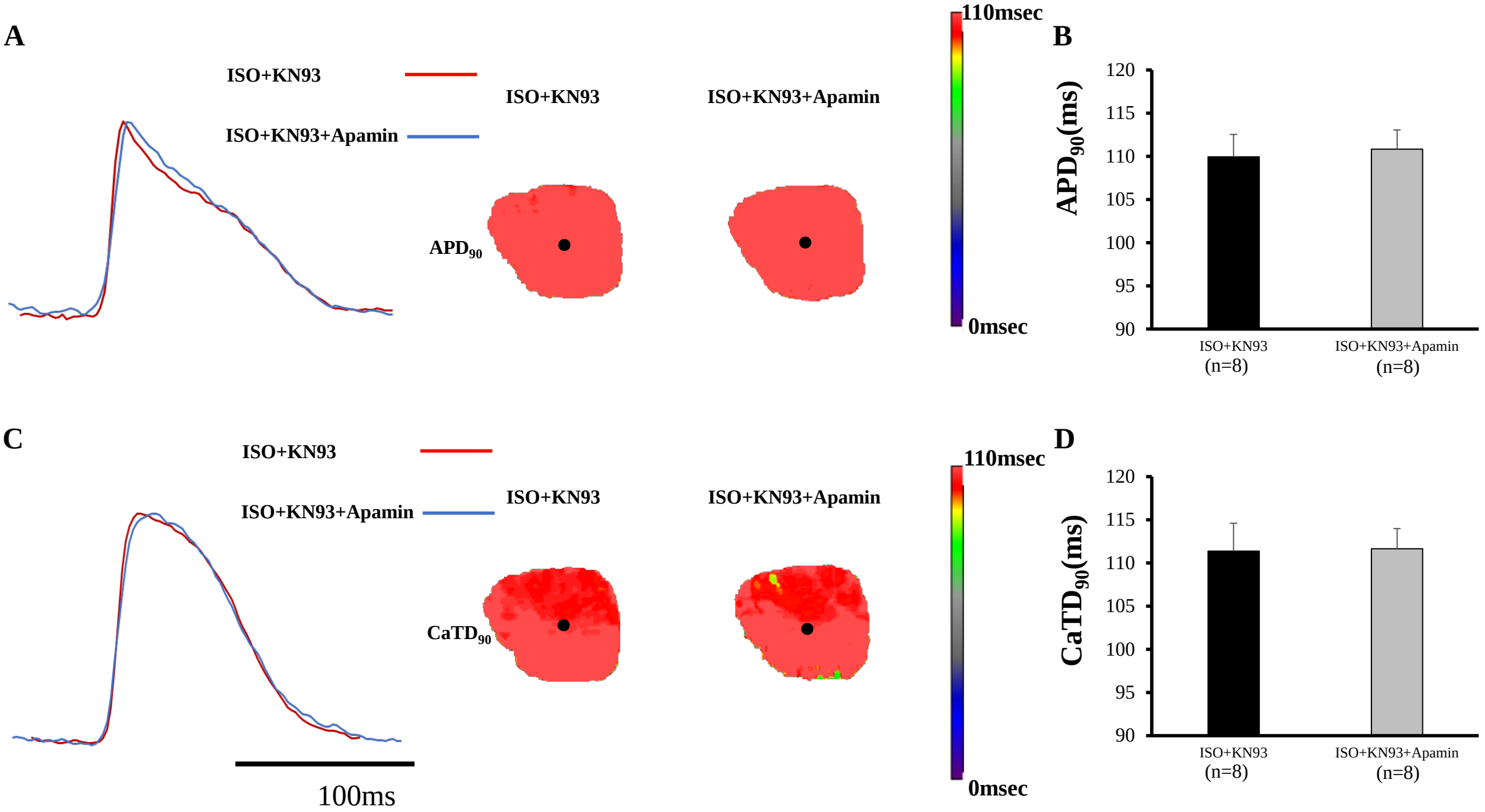
A
ISO+KN93
ISO+KN93+Apamin
ISO+KN93
ISO+KN93+Apamin
APD90
110msec
0msec
B
APD90(ms)
120
115
110
105
100
95
90
ISO+KN93
(n=8)
ISO+KN93+Apamin
(n=8)
C
ISO+KN93
ISO+KN93+Apamin
ISO+KN93
ISO+KN93+Apamin
CaTD90
110msec
0msec
100ms
D
CaTD90(ms)
120
115
110
105
100
95
90
ISO+KN93
(n=8)
ISO+KN93+Apamin
(n=8)